PCCP

Cite this: *Phys. Chem. Chem. Phys.*, 2012, **14**, 6577–6583

www.rsc.org/pccp

PAPER

Turing patterns in the chlorine dioxide–iodine–malonic acid reaction with square spatial periodic forcing

Daniel Feldman,[a] Raphael Nagao,[ab] Tamás Bánsági Jr.,[a] Irving R. Epstein[a] and Milos Dolnik*[a]

Received 28th November 2011, Accepted 9th March 2012
DOI: 10.1039/c2cp23779b

We use the photosensitive chlorine dioxide–iodine–malonic acid reaction–diffusion system to study wavenumber locking of Turing patterns to two-dimensional "square" spatial forcing, implemented as orthogonal sets of bright bands projected onto the reaction medium. Various resonant structures emerge in a broad range of forcing wavelengths and amplitudes, including square lattices and superlattices, one-dimensional stripe patterns and oblique rectangular patterns. Numerical simulations using a model that incorporates additive two-dimensional spatially periodic forcing reproduce well the experimental observations.

Introduction

Turing patterns (TP) are spatially periodic, stationary patterns that form in reaction–diffusion systems through a diffusion-driven instability.[1] This symmetry-breaking instability has been suggested as a possible mechanism for morphogenesis and employed to explain skin pattern generation in animals.[2] The first experimental verification of Turing's theoretical work was demonstrated in the chlorite–iodide–malonic acid (CIMA) reaction.[3] Since then, Turing patterns have been intensively studied and several other reaction–diffusion systems have been found that satisfy the conditions for TP formation. Chemical systems that produce TP include the thiourea–iodate–sulfite reaction[4] and the Belousov–Zhabotinsky reaction in a reverse microemulsion.[5,6]

After the experimental confirmation of TP in the CIMA reaction, attention initially focused on the spontaneously formed hexagonal and stripe patterns.[7–10] In the past decade, investigations of TP in reaction–diffusion systems have shifted to pattern formation in the presence of spatiotemporal forcing[11–13] and the imprinting of Turing patterns by strong illumination.[14–17] The majority of these studies utilize the photosensitive chlorine dioxide–iodine–malonic acid (CDIMA) reaction.[18] Illumination of the CDIMA reaction with white light results in the photodissociation of molecular iodine, which leads to the reduction of chlorine dioxide to chlorite and the oxidation of iodide ions to iodine.[19] Through these processes, the formation of TP can be effectively controlled, and this strategy has been employed to create unique initial conditions that lead to formation of novel Turing patterns. Stable rhombic and superlattice hexagonal patterns[14–16] were obtained when pattern formation was controlled by light projected through masks with rhombic and hexagonal geometries. Square superlattice TP were generated with simple square masks. Unlike the rhombic and superlattice hexagonal patterns, the square superlattice TP were found to be rather short-lived, as they evolved into labyrinthine patterns soon after the forcing was removed.[17] Square patterns emerge in a variety of experiments on nonequilibrium systems, including Faraday waves,[20,21] Marangoni–Bénard[22–24] and Rayleigh–Bénard convection,[25–28] as well as in dielectric barrier discharges,[29] but not in reaction–diffusion systems. The role of temporally constant, one-dimensional periodic forcing was recently investigated in thermal convection patterns[30] and in the Swift–Hohenberg model.[31,32] These studies show that this type of simple forcing can lead to resonance in two dimensions, resulting in a variety of wavenumber-locked patterns. Moreover, our recent results[33] reveal that resonant two-dimensional patterns can also be obtained in the CDIMA reaction–diffusion system with one-dimensional forcing by illumination. However, these two-dimensional resonant structures arise only in a very narrow range of forcing parameters and are quite rare with one-dimensional forcing. Most of the resonant patterns we obtained are aligned with the one-dimensional forcing and do not grow modes perpendicular to the direction of forcing.

In this study we investigate wavenumber-locking phenomena in TP in the CDIMA reaction–diffusion system under *two-dimensional* square spatially periodic forcing implemented as orthogonal sets of bright bands projected onto the reaction medium. In particular, we focus on the resonant patterns that emerge when the photosensitive system is weakly forced with two sets of orthogonal bright stripes. By applying this type of two-dimensional forcing, we investigate conditions under which square TP can develop and be stabilized in the CDIMA reaction–diffusion system. This is a particularly important

[a] *Department of Chemistry and Volen Center for Complex Systems, MS 015, Brandeis University, Waltham, MA 02454, USA. E-mail: dolnik@brandeis.edu*
[b] *Institute of Chemistry of São Carlos, University of São Paulo, CP 780, CEP 13560-970, São Carlos, SP, Brazil*

question, since it is well-known that square TP do not form spontaneously in systems of this type.[17,34] We also investigate other types of two-dimensional patterns that can emerge and be stabilized by "square" forcing when the forcing wavelength is either near to or far from the natural pattern wavelength.

Experimental

The experiments were carried out in a continuously-fed unstirred reactor (CFUR). The CFUR, which consisted of a 2% agarose gel (Fluka, thickness 0.3 mm, diameter 25 mm) and served as a working medium for the pattern formation, was in contact on one side with a continuously-fed stirred tank reactor (CSTR) and on the other side with an impermeable optical glass window through which the spatial forcing by illumination was applied. The CSTR was placed underneath the CFUR and served as a feeding chamber for the CFUR. The volume of the CSTR chamber was 2.7 mL. Three small magnetic stirring bars rotated at a constant speed of 1000 rpm to homogenize the reaction mixture in the CSTR compartment. The CFUR was separated from the CSTR compartment by two membranes: a cellulose nitrate membrane (Whatman, pore size 0.45 μm, thickness 0.12 mm) placed beneath the gel for enhanced contrast, and an anopore membrane (Whatman, pore size 0.2 μm, impregnated with 4% agarose gel, overall thickness 0.10 mm) to provide rigid support to the gel and to separate the CFUR from the intensively stirred feeding chamber. The reactor assembly was thermostated at 4 °C.

Three reagent solutions: (i) I_2 (Aldrich), (ii) a mixture of malonic acid (MA, Aldrich) and poly-(vinyl alcohol) (PVA, Aldrich, average molecular weight 9000–10000), and (iii) ClO_2 prepared as described in ref. 35 were fed into the CSTR by three peristaltic pumps (Rainin). The PVA is a binding agent for triiodide ions and also acts as a color indicator. It plays a key role in diminishing the effective diffusivity of iodide, which is essential to the formation of Turing patterns.[12] The initial concentrations of reactants (at the instant of mixing in the feeding chamber) were the same in all experiments: $[I_2] = 0.4$ mM, $[MA] = 1.8$ mM, $[ClO_2] = 0.14$ mM, and $[PVA] = 10$ g L^{-1}. Each of the input solutions contained 10 mM sulfuric acid. The residence time of the reagents in the CSTR was 160 s.

The spatial forcing was implemented by projecting two-dimensional grayscale images of squares on the working medium with a PC-controlled DLP projector (Dell 1510X). A CCD camera (Pulnix) equipped with a Hamamatsu camera control unit was used to record images of TP. Snapshots were taken in ambient light (0.6 mW cm^{-2}), with no image projected on the CFUR. In this study we investigated resonant pattern formation employing forcing wavelengths, λ_F, between $0.6\lambda_P$ and $2.5\lambda_P$, where λ_P is the intrinsic wavelength of the Turing patterns in the absence of forcing.

Experimental results

It typically took several hours from the start of feeding the CSTR with reactant solutions for TP to spontaneously develop and to become stationary. Under the above reaction conditions, we obtained labyrinthine patterns composed of randomly oriented stripes in the presence of a few spots (Fig. 1a). After the TP became stationary, we took a snapshot of the pattern and evaluated the pattern wavelength from its Fourier spectrum. The average wavelength of spontaneously developed patterns in our experiments was $\lambda_P = 0.40 \pm 0.03$ mm. The pattern was then illuminated by strong, homogeneous white light (I_{max} = 101 mW cm^{-2}) for 2 min in order to suppress the TP and to create uniform initial conditions.

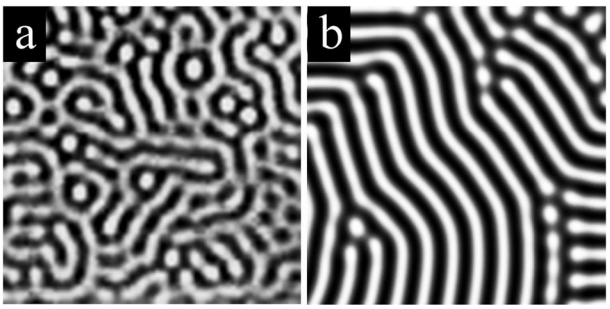

Fig. 1 Labyrinthine Turing patterns in the unforced CDIMA reaction–diffusion system. (a) Results of experiments, snapshot area 5 × 5 mm. For reaction conditions, see text. (b) Results of simulations with model (1): $a = 12$, $b = 0.32$, $d = 1$, and $\sigma = 50$. System size is 84 × 84 space units (grid 168 × 168). Black represents high concentration of $[SI_3^-]$.

After the pattern suppression, spatial forcing was applied by projecting images composed of grayscale squares. The squares were produced by overlaying two perpendicular sets of stripes with the same wavelength, λ_F. Each set of bands had a square-wave, or "on–off," intensity profile in the normal direction; therefore the superposition of the two sets created squares of equal size with three different grayscale levels. During forcing, the maximum light intensity, I_{max}, was applied through the square areas where the bright stripes intersect (Fig. 2a). At the intersections of the black bands, the intensity was zero. Medium intensity light, $I_{int} = I_{max}/2$, was cast on the areas where perpendicular stripes of "on" and "off" overlapped.

As reported previously,[33] when the intensity of the forcing was very low ($I_{max} < 2.0$ mW cm^{-2}) the evolved patterns were similar to the spontaneously formed ones. When the light intensity was increased above 2.0 mW cm^{-2}, the influence of spatial periodic forcing on the pattern formation process became noticeable. Forcing just above the threshold can result in TP that differ from the applied mask. There was often no locking between the forcing wavelength and the wavelength of the patterns that developed in the presence of illumination. Typically, above I_{max} = 7.0 mW cm^{-2} the illumination was strong enough that images projected on the CFUR became completely imprinted. In general, the symmetric "square" patterns that formed under the influence of illumination were stable only as long as the forcing was maintained, irrespective of the forcing strength. In a few cases, when the wavelength of the forcing was equal to or near the intrinsic wavelength, forced stripe patterns persisted after the illumination was switched off.

Two-dimensional forcing led to formation of TP that displayed resonant behavior within a large domain of forcing wavelength, λ_F, and forcing amplitude, I_{max}, as illustrated in Fig. 3. Two-dimensional 1 : 1 locking between the forcing image and the TP was found when λ_F was close to the intrinsic pattern wavelength (Fig. 2 and 3a). However, for lower light intensities

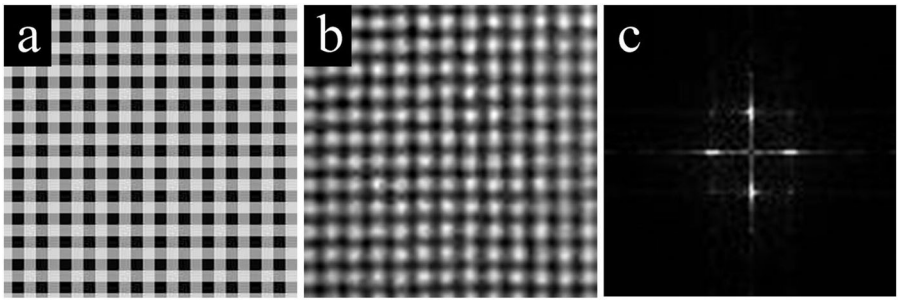

Fig. 2 Resonant Turing pattern formation in the CDIMA reaction with two-dimensional spatial forcing—experimental results. (a) An image projected on the surface of the gel. (b) Turing pattern developed under the illumination shown in (a). Wavelength of forcing in each spatial dimension is $\lambda_F = 0.9\lambda_P$, and amplitude of forcing, $I_{max} = 4.0$ mW cm^{-2}. Snapshot area is 5 mm × 5 mm and the snapshot was taken 2 h after the start of forcing. (c) 2D-FFT of the pattern shown in (b). The displayed wavenumber domain is ±9.4 mm^{-1} × ±9.4 mm^{-1}.

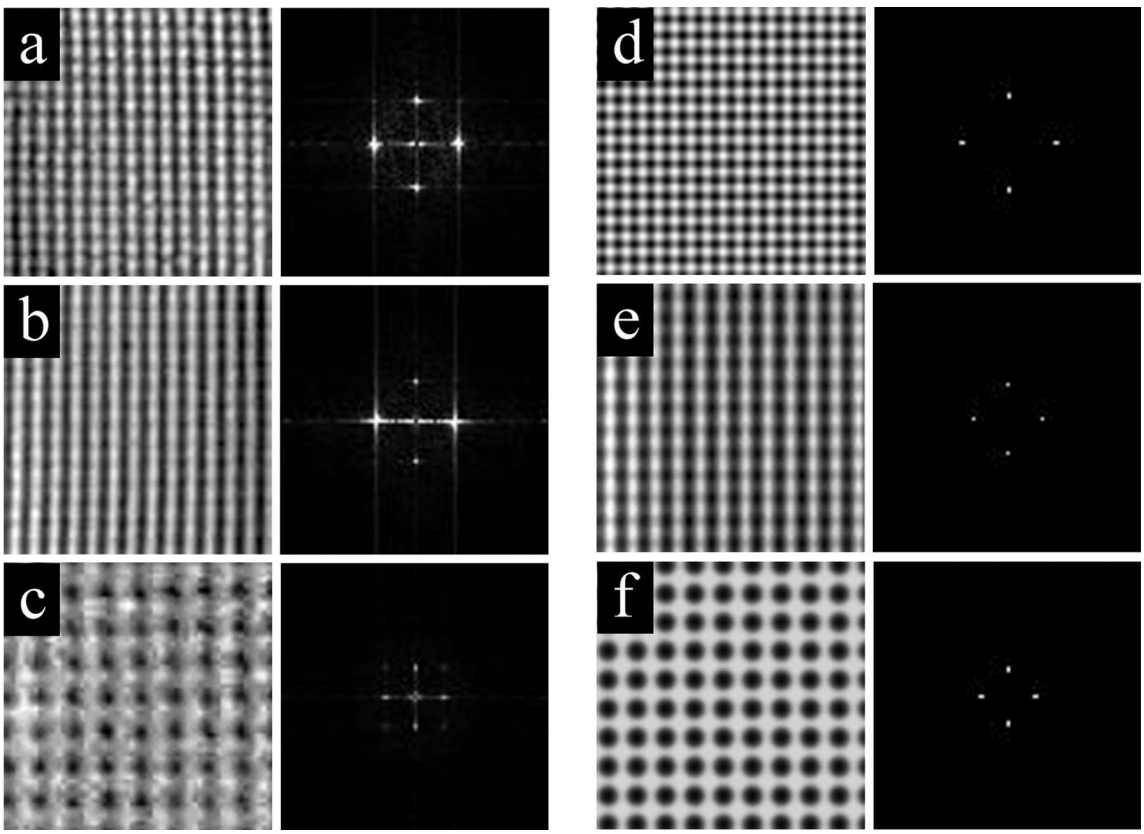

Fig. 3 1 : 1 resonant Turing patterns in the CDIMA reaction with corresponding 2D Fourier spectra. (a–c) Experimental results, forcing parameters: (a) $\lambda_F = 0.7\lambda_P$, $I_{max} = 10$ mW cm^{-2}, (b) $\lambda_F = \lambda_P$, $I_{max} = 4.0$ mW cm^{-2}, (c) $\lambda_F = 1.4\lambda_P$, $I_{max} = 10$ mW cm^{-2}. Snapshot area is 5 mm × 5 mm and Fourier spectra display wavenumber domain ±9.4 mm^{-1} × ±9.4 mm^{-1}. Snapshots were taken 2 h after the start of forcing. (d–f) Results of simulations, forcing parameters: (d) $\lambda_F = 0.7\lambda_P$, $w_{max} = 0.7$, (e) $\lambda_F = \lambda_P$, $w_{max} = 0.2$, (f) $\lambda_F = 1.3\lambda_P$, $w_{max} = 0.5$. The size of the system shown is 84 s.u. × 84 s.u. (grid size 168 × 168), and Fourier spectra display wavenumber domain ±0.56 s.u.$^{-1}$ × ±0.56 s.u.$^{-1}$.

($I_{max} < 4.0$ mW cm^{-2}) stripes were favored over square arrangements of spots. The stripe formation reflected the two principal directions of the masks, resulting in patterns with several wavelengths, each consisting of either a horizontally or vertically oriented stripe TP. An example of the latter is presented in Fig. 3b. The Fourier spectrum of the pattern (Fig. 3b) supports this visual assessment, with two major peaks in the horizontal direction. In the following, we use the terms resonant pattern and wavenumber locking for any pattern that displays resonant behavior in at least one spatial dimension.

As the forcing amplitude was increased, 1 : 1 resonant patterns appeared over a wider range of forcing wavelength. For $I_{max} = 10$ mW cm^{-2}, resonant patterns were found for $0.7\lambda_P < \lambda_F < 1.7\lambda_P$. This expansion was accompanied by a change in symmetry of the TP. Stripes gave way to square patterns, as illustrated by the Fourier spectrum (Fig. 3c) composed of four peaks corresponding to a square lattice.

In addition to the large 1 : 1 resonance domain, we also observed 1 : 2 wavenumber locking behavior. Resonant patterns in this regime displayed different forms of square lattices,

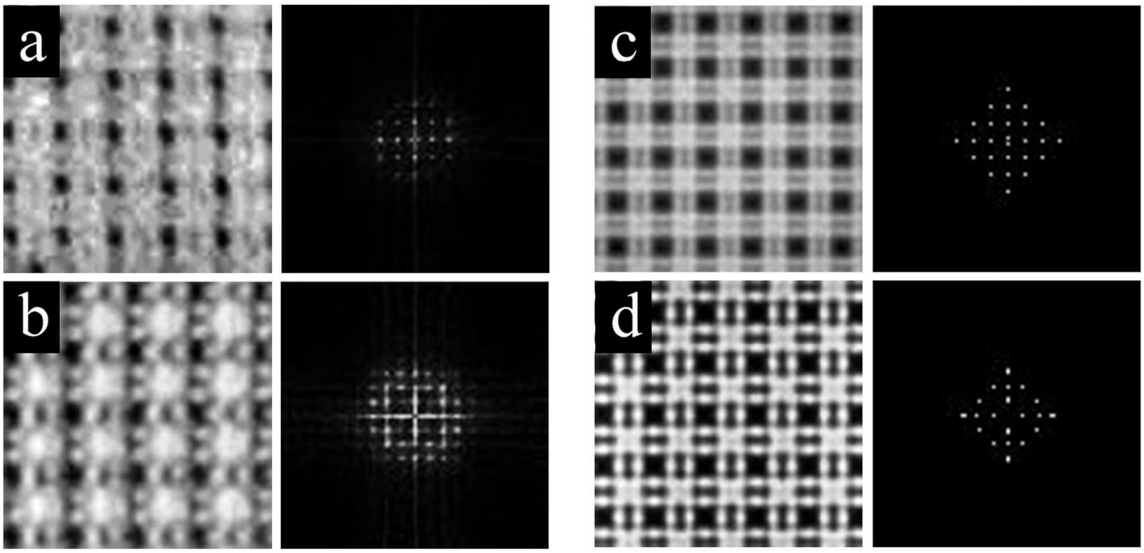

Fig. 4 1 : 2 resonant Turing patterns in the CDIMA reaction with corresponding 2D Fourier spectra. (a, b) Experimental results, forcing parameters: (a) $\lambda_F = 2.0\lambda_P$, $I_{max} = 8.2$ mW cm^{-2}, (b) $\lambda_F = 2.5\lambda_P$, $I_{max} = 9.4$ mW cm^{-2}. Snapshots were taken 2 h after the start of forcing. (c, d) Results of simulations, forcing parameters: (c) $\lambda_F = 2.0\lambda_P$, $w_{max} = 1.0$, (d) $\lambda_F = 2.3\lambda_P$, $w_{max} = 0.7$. Size of the system as in Fig. 3.

depending on the wavelength of forcing. In the center of this resonant domain with $\lambda_F \approx 2\lambda_P$, the pattern consisted of pairs of stripes in both the horizontal and vertical directions. These stripes were formed by splitting each broad, bright band of illumination into two narrower stripes (Fig. 4a and b). Above $\lambda_F = 2\lambda_P$, spots developed in the areas illuminated with intermediate light intensity around the brightest-lit squares. In the Fourier spectra of these resonant 1 : 2 wavenumber-locked patterns, the four peaks at small wavenumber correspond to the forcing wavenumber, k_F. Another tetrad of peaks appears at $2k_F$, which corresponds to the average wavelength of the forced pattern. Both spectra contain an additional eight peaks that can be attributed to resonance between the k_F wavenumber of the spatial forcing and the k_P wavenumber of the forced pattern. Harmonics of the forcing wavelength are present in the spectra of 1 : 2 wavenumber-locked patterns (Fig. 4).

Our experiments revealed that resonant behavior is not confined to the 1 : 1 and 1 : 2 wavenumber locking regimes. Near these major resonant domains we also observed other symmetric resonant TP. Fig. 5a shows resonant patterns obtained when the wavelength of forcing was close to half the natural wavelength. Within a relatively narrow range of forcing parameters (λ_F, I_{max}) a different arrangement of square TP was observed: white spots arranged in a square lattice. The lattice orientation was rotated by $\pi/4$ with respect to the principal axes of the applied mask, and the distance between neighboring spots in the lattice was $2\lambda_F$. The corresponding Fourier spectrum displayed major peaks at $k_F/\sqrt{2}$ from the origin or at $k_y = k_x = \pm k_F/2$ ($k_y, k_x \neq 0$), which indicates a 2 : 1 resonance.

Slightly below $\lambda_F = 2\lambda_P$, the unit cells of the dominant TP were squares with a spot in the center (Fig. 6a). The Fourier spectrum of this superlattice structure resembles those of patterns in the 1 : 2 wavenumber-locking regime.

A different type of resonant pattern was found in the vicinity of $\lambda_F = 1.2\lambda_P$ (Fig. 7a). This forced pattern was composed of short, bright segments with their normal vector at 45° to the principal directions of the mask. This *oblique rectangular* arrangement is detected in the Fourier spectrum as two peaks in a diagonal direction with respect to the forcing, in addition to the four modes at k_F representing forcing. This resonant pattern can be considered as a special case of 1 : 1 wavenumber locking. A unique symmetric pattern was observed for $\lambda_F = 2\lambda_P$ and relatively low intensity, $I_{max} = 4.6$ mW cm^{-2} (Fig. 7b). It was composed of elongated black eyes and spots arranged on a square lattice.

Our experimental results are summarized in the phase plane diagram, Fig. 8a. The majority of patterns found are square patterns with 1 : 1 and 1 : 2 wavenumber locking resonances. We have also found 2 : 1 square resonant TP in a relatively narrow range of forcing parameters. Non-resonant and

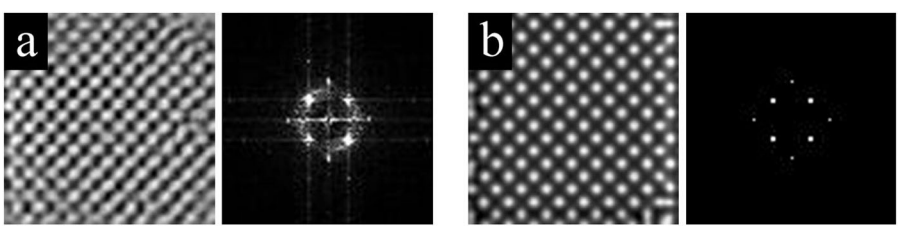

Fig. 5 2 : 1 resonant Turing patterns in the CDIMA reaction with corresponding 2D Fourier spectra. (a) Experimental results, forcing parameters: $\lambda_F = 0.6\lambda_P$, $I_{max} = 7.6$ mW cm^{-2}. Snapshots were taken 2 h after the start of forcing. (b) Results of simulations, forcing parameters: $\lambda_F = 0.7\lambda_P$, $w_{max} = 0.2$ and $b = 34$. Size of the system as in Fig. 3.

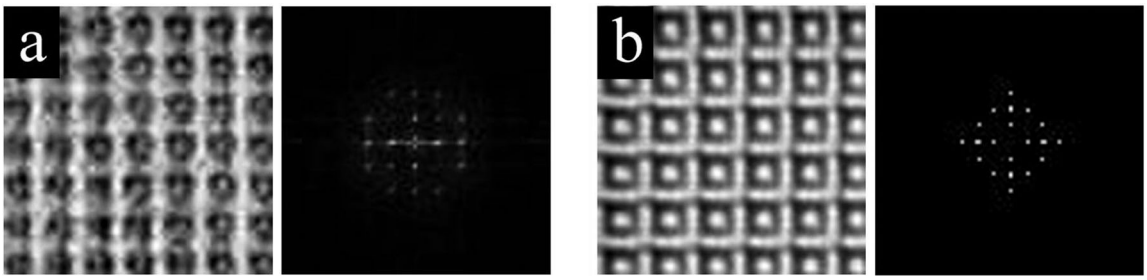

Fig. 6 Forced Turing pattern found between 1 : 1 and 1 : 2 resonant domains. (a) Experimental results, forcing parameters $\lambda_F = 1.7\lambda_P$, $I_{max} = 5.8$ mW cm^{-2}. Snapshots were taken 2 h after the start of forcing. (b) Results of simulations, forcing parameters: $\lambda_F = 2.1\lambda_P$, $w_{max} = 0.4$. Size of the system as in Fig. 3.

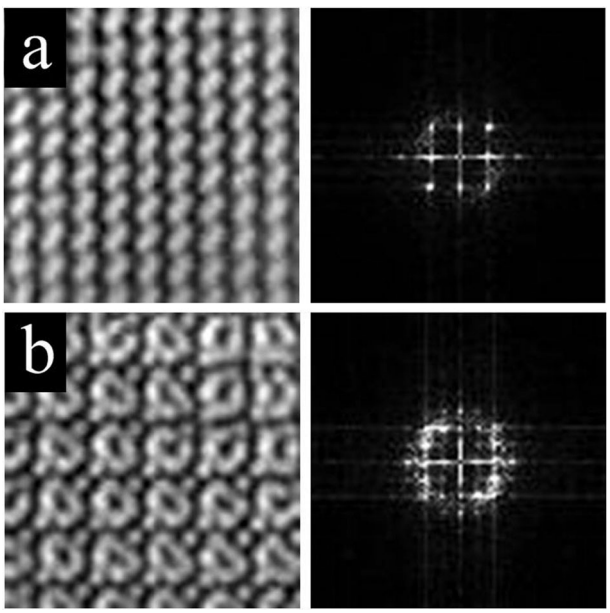

Fig. 7 Forced Turing patterns—experimental results. Forcing parameters: (a) $\lambda_F = 1.2\lambda_P$ and $I_{max} = 8.2$ mW cm^{-2}. (b) $\lambda_F = 2.0\lambda_P$ and $I = 4.6$ mW cm^{-2}. Snapshots were taken 2 h after the start of forcing. Size of the system as in Fig. 3.

asymmetric patterns were found in our experiments for weak forcing and are shown in the diagram as filled circles.

Model

We employed the Lengyel–Epstein[36] model with the influence of light incorporated as an additive term.[14] The evolution equations corresponding to our experiments are:

$$\frac{\partial u}{\partial t} = a - u - 4\frac{uv}{1+u^2} - w(x,y) + \nabla^2 u$$
$$\frac{\partial v}{\partial t} = \sigma\left[b\left(u - \frac{uv}{1+u^2} + w(x,y)\right) + d\nabla^2 v\right]. \quad (1)$$

Here u and v are the dimensionless concentrations of $I^-$and ClO_2^- ions, respectively; a, b, d, σ are dimensionless parameters. The effect of illumination is included through the term $w(x,y)$, which is proportional to the rate of the photochemical reaction that produces ClO_2^- and consumes I^-. To reproduce the intensity profile of the masks used in our experiments, we

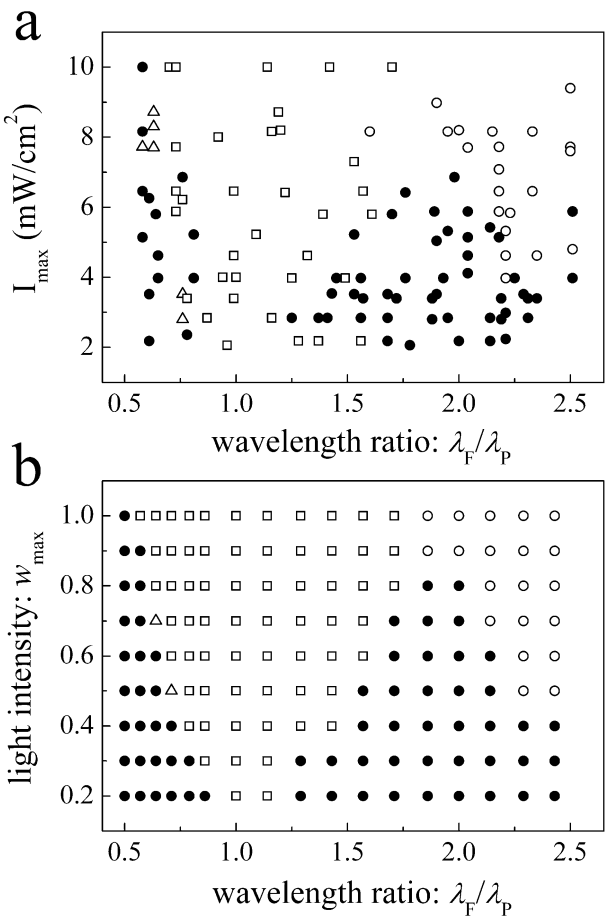

Fig. 8 Phase diagram of Turing patterns in the CDIMA reaction under two-dimensional square spatial forcing. (a) Experimental results, (b) results of simulations. Symbols: 1 : 1 locking (□), 1 : 2 locking (○), 2 : 1 locking (Δ), and other patterns (●).

assign three different values, w_{max}, w_{int}, and 0, corresponding to I_{max}, I_{int}, and 0, respectively, to $w(x,y)$ as a function of the spatial x and y-coordinates (Fig. 2a). Unless otherwise noted, the parameters used in our simulations are: $a = 12$, $b = 0.32$, $d = 1$, and $\sigma = 50$, for which, in the absence of forcing, labyrinthine TP similar to those seen in experiments at ambient light are obtained (Fig. 1b).

Our two dimensional simulations were performed with 256 × 256 grid points at a spacing of 0.5 space units (s.u.) surrounded by no-flux boundaries. We employed the explicit

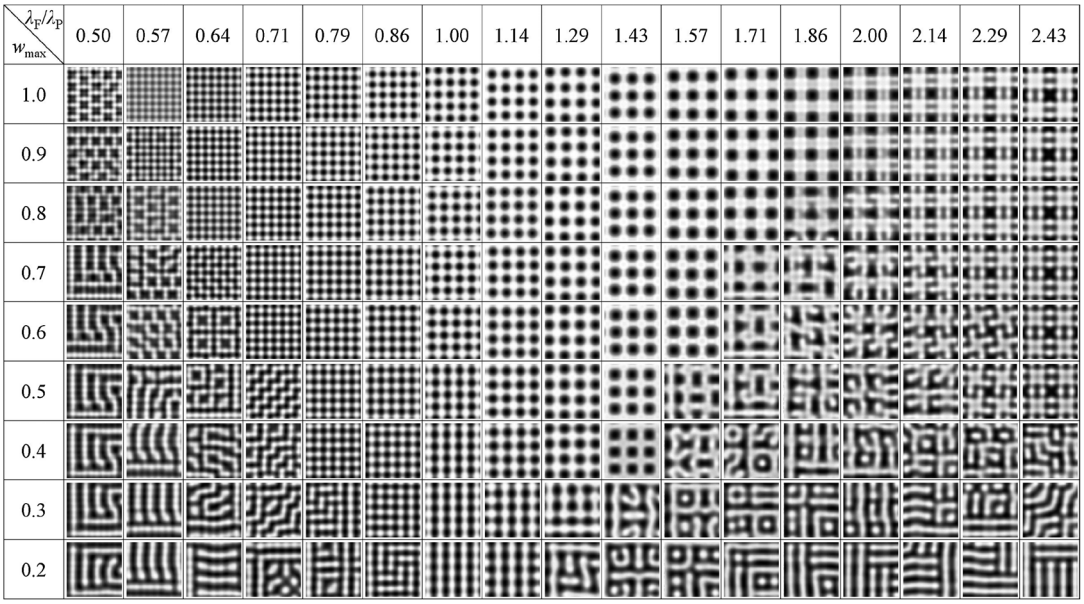

Fig. 9 Snapshots of Turing patterns in the CDIMA reaction under two-dimensional square spatial forcing—results of simulations. Fixed parameters: $a = 12$, $b = 0.32$, $d = 1$, and $\sigma = 50$. The size of each snapshot is 32×32 space units (64×64 grid size).

Euler method with a time step of 0.001 and used a 9-point stencil to compute the Laplacians. As initial conditions, both variables were set to their unstable steady-state values and a small (1% of the steady state value) random fluctuation was added to u at each grid point.

Numerical results

We investigated numerically TP formation in the λ_F *vs.* w_{max} parameter plane with forcing wavelengths $0.5\lambda_P \leq \lambda_F \leq 2.4\lambda_P$ and forcing amplitudes $0.2 \leq w_{max} \leq 1.0$. In most cases we obtained results qualitatively similar to the experiments. To facilitate comparison of the experimental and numerical results, we show the snapshots of patterns obtained in our simulations next to the experimentally observed TP (Fig. 3–6). The results of the simulations are summarized in the phase diagram in Fig. 8b. Cropped snapshots of Turing patterns corresponding to this phase diagram are displayed in Fig 9.

In general, when the forcing amplitude, w_{max}, was below 0.2, the forcing was very weak, and non-resonant asymmetric TP were obtained. However, when the forcing wavelength was close to the intrinsic wavelength, we obtained resonant stripe patterns even for $w_{max} = 0.1$. With increasing forcing amplitude, the domain of wavenumber-locked 1 : 1 resonant TP gradually broadened, and the 1 : 1 resonant domain spanned $\lambda_F = 0.6\lambda_P$ to $1.7\lambda_P$ for $w_{max} = 1$ (Fig. 8b). The Fourier spectra of the patterns in this regime were comprised of either two or four peaks, depending on the forcing amplitude. Our simulations also confirmed the existence of 1 : 2 resonant patterns. The domain with the 1 : 2 resonance was smaller than the 1 : 1 domain, and the simulations gave patterns with more resolution and details, as shown in Fig. 4c and d. The main modes in the corresponding Fourier spectra were found for wavenumbers similar to those in the 1 : 2 resonant patterns obtained in experiments. The harmonic modes were more distinct in the Fourier spectra of the simulated patterns. The resonant 2 : 1 wavenumber locking TP were also found numerically (Fig 5b) along with the superlattice pattern observed between the 1 : 1 and 1 : 2 regimes.

In an effort to simulate the experimental patterns shown in Fig. 7, we varied the parameter b over a relatively wide range (from 0.20 to 0.36) while keeping all other parameters (a, d and σ) constant, but we were not successful to find matching patterns. However, we were able to find the negative of the pattern shown in Fig 7a for $b = 0.24$. Some of the discrepancies between experimental and numerical results might be due to imperfections in our image projection on the working area of the gel. Even though the projected images were always focused on the gel surface, the light had to pass through the thermostated water bath in which the reactor was submerged. This could result in light scattering of a projected image and imperfections in pattern forcing. On the other hand, several unique patterns were obtained only in simulations but we did not observe these patterns in our experiments. To test and verify that the imperfection in the image projection may influence the pattern formation, we performed additional simulations using a $w(x,y)$ profile with rounded edges. We noticed that some of these unique patterns diminished in our simulations when slight sinusoidal deviations were applied to the sharp on–off $w(x,y)$ profile.

Discussion and conclusions

Our study illustrates that square spatial forcing may produce a variety of square TP. These patterns are only sustained while the forcing is maintained, in accord with ample experimental observations and theoretical findings,[8] which indicate that stripes and hexagonally arranged spots are the only basic stable structures in reaction–diffusion systems. Although both types can serve as building blocks of superlattice patterns, their inherent symmetry remains unchanged in those complex structures.

As in previous work with one-dimensional forcing,[33] this study reveals that square spatial forcing implemented as perpendicular sets of bright stripes produces patterns with wavenumbers locked with the forcing wavenumber $k_x = k_y = k_F$ in both principal directions. At relatively weak amplitudes of forcing, TP align with either one of the sets, *i.e.*, undergo *one-dimensional locking to two-dimensional forcing*. Also, a special type of *diagonal locking* occurs within a small regime in the 1 : 1 resonance domain, resulting in oblique rectangular TP. Note that, in contrast to the one-dimensional case, where "natural" hexagonal patterns were induced by forcing at appropriate wavelengths, no evidence is found here for induction of hexagonal patterns by our two-dimensional forcing.

We also observe that patterns with 1 : 2 wavenumber locking resonance are found in a larger domain in the forcing amplitude *vs.* forcing wavelength phase plane relative to the size of the corresponding resonant domain for one-dimensional forcing.[33] The expansion of this domain indicates an increase in stability caused by the new dimension of forcing. The square superlattice structures presented in Fig. 5a display similarities with those found in dielectric barrier discharge,[29] which underlines the resemblance between patterns arising in disparate nonequilibrium systems.

The light sensitivity in the CDIMA reaction and its model is additive. Therefore our findings cannot be directly generalized and applied to other systems or models in which stationary patterns emerge due to multiplicative forcing. However, resonant TP, such as oblique and rectangular patterns, that develop as a result of one-dimensional multiplicative forcing,[31,32] have been also found in the CDIMA reaction–diffusion system in a narrow range of forcing parameters where the unforced stripe pattern is in close proximity to the domain of hexagonal patterns.[33] Therefore, one might expect to find similar resonant patterns in the stripe domain induced by this type of two-dimensional forcing when the nature of forcing is multiplicative.

Acknowledgements

This work was supported by the National Science Foundation under grant CHE-1012428 and the U.S.-Israel Binational Science Foundation. R.N. (# 0337110) acknowledges CAPES (Coordenação de Aperfeiçoamento de Pessoal de Nível Superior) for financial support.

References

1 A. Turing, *Philos. Trans. R. Soc. London, Ser. B*, 1952, **37**, 237.
2 J. D. Murray, *Mathematical Biology*, Springer, Berlin, 1989.
3 V. Castets, J. Boissonade, E. Dulos and P. De Kepper, *Phys. Rev. Lett.*, 1990, **64**, 2953.
4 J. Horváth, I. Szalai and P. De Kepper, *Science*, 2009, **324**, 772.
5 V. K. Vanag and I. R. Epstein, *Phys. Rev. Lett.*, 2001, **87**, 228301.
6 T. Bánsági Jr., V. K. Vanag and I. R. Epstein, *Science*, 2011, **331**, 1309.
7 Q. Ouyang and H. L. Swinney, *Nature*, 1991, **352**, 610.
8 R. Kapral and K. Showalter, *Chemical Waves and Patterns*, Kluwer, Dordrecht, 1995.
9 I. R. Epstein and J. A. Pojman, *An Introduction to Nonlinear Chemical Dynamics*, Oxford, New York, 1998.
10 B. Rudovics, E. Barillot, P. W. Davies, E. Dulos, J. Boissonade and P. De Kepper, *J. Phys. Chem. A*, 1999, **103**, 1790.
11 S. Rüdiger, D. G. Míguez, A. P. Muñuzuri, F. Sagués and J. Casademunt, *Phys. Rev. Lett.*, 2003, **90**, 128301.
12 D. G. Míguez, E. M. Nicola, A. P. Muñuzuri, J. Casademunt, F. Sagués and L. Kramer, *Phys. Rev. Lett.*, 2004, **93**, 048303.
13 D. G. Míguez, V. Perez-Villar and A. P. Muñuzuri, *Phys. Rev. E: Stat. Phys., Plasmas, Fluids, Relat. Interdiscip. Top.*, 2005, **71**, 066217.
14 G. H. Gunaratne, Q. Ouyang and H. L. Swinney, *Phys. Rev. E: Stat. Phys., Plasmas, Fluids, Relat. Interdiscip. Top.*, 1994, **50**, 2802.
15 I. Berenstein, M. Dolnik, A. M. Zhabotinsky and I. R. Epstein, *J. Phys. Chem. A*, 2003, **107**, 4428.
16 I. Berenstein, L. F. Yang, M. Dolnik, A. M. Zhabotinsky and I. R. Epstein, *J. Phys. Chem. A*, 2005, **109**, 5382.
17 L. Yang, M. Dolnik, A. M. Zhabotinsky and I. R. Epstein, *Chaos*, 2006, **16**, 037114.
18 I. Lengyel, G. Rábai and I. R. Epstein, *J. Am. Chem. Soc.*, 1990, **112**, 4606.
19 A. P. Muñuzuri, M. Dolnik, A. M. Zhabotinsky and I. R. Epstein, *J. Am. Chem. Soc.*, 1999, **121**, 8065.
20 A. Kudrolli and J. P. Gollub, *Physica D (Amsterdam)*, 1996, **97**, 133.
21 P. B. Umbanhowar, F. Melo and H. L. Swinney, *Physica A (Amsterdam)*, 1998, **249**, 1.
22 M. F. Schatz, S. J. VanHook, W. D. McCormick, J. B. Swift and H. L. Swinney, *Phys. Fluids*, 1999, **11**, 2577.
23 K. Nitschke and A. Thess, *Phys. Rev. E: Stat. Phys., Plasmas, Fluids, Relat. Interdiscip. Top.*, 1995, **52**, R5772.
24 W. A. Tokaruk, T. C. A. Molteno and S. W. Morris, *Phys. Rev. Lett.*, 2000, **84**, 3590.
25 J. L. Rogers, M. F. Schatz, O. Brausch and W. Pesch, *Phys. Rev. Lett.*, 2000, **85**, 4281.
26 J. L. Rogers, W. Pesch, O. Brausch and M. F Schatz, *Phys. Rev. E: Stat. Phys., Plasmas, Fluids, Relat. Interdiscip. Top.*, 2005, **71**, 066214.
27 K. M. S. Bajaj, J. Liu, B. Naberhuis and G. Ahlers, *Phys. Rev. Lett.*, 1998, **81**, 806.
28 J. J. Sánchez-Álvarez, E. Serre, E. Crespo del Arco and F. H. Busse, *Phys. Rev. E: Stat. Phys., Plasmas, Fluids, Relat. Interdiscip. Top.*, 2005, **72**, 036307.
29 L. Dong, W. Fan, Y. He, F. Liu, S. Li, R. Gao and L. Wang, *Phys. Rev. E: Stat. Phys., Plasmas, Fluids, Relat. Interdiscip. Top.*, 2006, **73**, 066206.
30 G. Seiden, S. Weiss, J. H. McCoy, W. Pesch and E. Bodenschatz, *Phys. Rev. Lett.*, 2008, **101**, 214503.
31 R. Manor, A. Hagberg and E. Meron, *New J. Phys.*, 2009, **11**, 063016.
32 R. Manor, A. Hagberg and E. Meron, *Europhys. Lett.*, 2008, **83**, 1005.
33 M. Dolnik, T. Bánsági Jr., S. Ansari, I. Valent and I. R. Epstein, *Phys. Chem. Chem. Phys.*, 2011, **13**, 12578.
34 L. F. Yang, A. M. Zhabotinsky and I. R. Epstein, *Phys. Rev. Lett.*, 2004, **92**, 1980303.
35 *Handbook of Preparative Inorganic Chemistry*, ed. G. Brauer, Academic, New York, 2nd edn, 1963.
36 I. Lengyel and I. R. Epstein, *Science*, 1991, **251**, 650.